A Naturally Fluorescent *Mgp* Transgenic Mouse for Angiogenesis and Glaucoma Longitudinal Studies

Priyadarsini Asokan,[1] Rajendra N. Mitra,[1] Ramesh Periasamy,[1] Zongchao Han,[1,2] and Teresa Borrás[1,3]

[1]Department of Ophthalmology, University of North Carolina School of Medicine, Chapel Hill, North Carolina, United States
[2]UNC Eshelman School of Pharmacy, University of North Carolina, Chapel Hill, North Carolina, United States
[3]Gene Therapy Center, University of North Carolina, Chapel Hill, North Carolina, United States

Correspondence: Teresa Borrás, Department of Ophthalmology, Gene Therapy Center, University of North Carolina School of Medicine, 4109C Neuroscience Research Building CB 7041, 105 Mason Farm Road, Chapel Hill, NC 27599-7041, USA; tborras@med.unc.edu.

Submitted: September 18, 2017
Accepted: January 2, 2018

Citation: Asokan P, Mitra RN, Periasamy R, Han Z, Borrás T. A naturally fluorescent *Mgp* transgenic mouse for angiogenesis and glaucoma longitudinal studies. *Invest Ophthalmol Vis Sci*. 2018;59:746–756. https://doi.org/10.1167/iovs.17-22992

Purpose. Our goal was to generate and characterize a new mouse model in which only angiogenesis- and glaucoma-relevant tissues would be naturally fluorescent. The Matrix Gla (MGP) gene is highly expressed in vascular smooth muscle cells (VSMC) and trabecular meshwork (TM). We sought to direct our *Mgp*-Cre.KI mouse recombinase to VSMC/TM cells to produce their longitudinal fluorescent profiles.

Methods. Homozygous *Mgp*-Cre.KI mice were crossed with Ai9 homozygous reporter mice harboring a *loxP*-flanked STOP cassette preventing transcription of a DsRed fluorescent protein (tdTomato). The F1 double-heterozygous (*Mgp*-tdTomato) was examined by direct fluorescence, whole mount, histology, and fundus photography. Custom-made filters had 554/23 emission and 609/54 exciter nanometer wavelengths. Proof of concept of the model's usefulness was conducted by inducing guided imaging laser burns. Evaluation of a vessel's leakage and proliferation was followed by noninvasive angiography.

Results. The *Mgp*-tdTomato mouse was viable, fertile, with normal IOP and ERG. Its phenotype exhibited red paws and snout (cartilage expression), which precluded genotyping. A fluorescent red ring was seen at the limbus and confirmed to be TM expression by histology. The entire retinal vasculature was red fluorescent (VSMC) and directly visualized by fundus photography. Laser burns on the *Mgp*-tdTomato allowed separation of leakiness and neovascularization evaluation parameters.

Conclusions. The availability of a transgenic mouse naturally fluorescent in glaucoma-relevant tissues and retinal vasculature brings the unique opportunity to study a wide spectrum of single and combined glaucomatous conditions in vivo. Moreover, the *Mgp*-tdTomato mouse provides a new tool to study mechanisms and therapeutics of retinal angiogenesis longitudinally.

Keywords: matrix Gla, knockin, Cre mice, fluorescent *loxP* reporter mice, trabecular meshwork, retinal vasculature

Matrix Gla (MGP), a potent inhibitor of mineralization, is a secreted 10.6-kDa protein known to be expressed at high levels in cartilage chondrocytes[1] and in vascular smooth muscle cells (VSMCs) of the tunica media of the blood vessels' wall.[2,3] Using first microarrays on perfused postmortem human anterior segments, and then molecular analyses, we had reported that MGP was also highly expressed in the trabecular meshwork (TM) of the eye.[4] Its expression there was regulated by IOP[5–7] and its levels were lower in TMs from glaucomatous patients.[8] MGP has since been recognized as a TM cell marker, including on differentiating stem cells' studies.[9,10]

Crosses of our generated *Mgp*-Cre.KI mouse with a floxed *LacZ* reporter mouse validated the specific localization of *Mgp* to the mouse TM and further revealed a second expression site, the peripapillary sclera.[11] The presence of *Mgp* in these glaucoma-relevant sites, together with the known function of MGP as a calcification inhibitor, led us to put forward the concept that calcification might have a major role in anterior and posterior segment stiffness leading to glaucoma, with *MGP* acting as its master regulator gene.[9]

Independently, the role of MGP in the vascular system has been studied in mice. Ablation of *Mgp* in mice results in massive arterial calcification, vessel rupture, and death of the animal at approximately 5 to 6 weeks of age.[12] MGP has further been shown to stimulate VEGF expression through TGFβ1 in bovine aortic endothelial cells.[13] MGP is activated by a vitamin K–dependent γ-carboxylase enzyme, and experiments in our laboratory have shown that the MGP of the human TM is active.[8,14]

Given the relevance of the retinal vasculature in angiogenesis and glaucoma, together with the availability of imaging technology to evaluate fluorescent eye structures, here we sought to determine whether our genetic tools would also be adequate to study the eye's vascular network noninvasively. Crossing our *Mgp*-Cre.KI mice[11] with floxed reporter mice (The Jackson Laboratory, Bar Harbor, ME, USA) offers the unique possibility of obtaining distinct transgenic mouse lines that are labeled with the corresponding fluorescent reporter gene on the tissues where *Mgp* is specifically expressed. Because the Cre recombinase gene in

the *Mgp*-Cre.KI mouse is under the control of the entire coding and noncoding regulatory regions of *Mgp*, the labeled cells represent a true expression profile of the gene.

In our first study, in which we used a *LacZ* reporter mouse, we focused on color-stained, static histologic sections of the eye on the death of the animal. In the present study, we aimed to visualize not only the TM, but potential naturally fluorescent retinal and choroidal vasculatures in vivo. For that, we crossed the *Mgp*-Cre.KI transgenic mouse with a DsRed fluorescent floxed reporter line (tdTomato), and evaluated the *Mgp* tissue–specific fluorescence of the F1 (*Mgp*-tdTomato) by noninvasive imaging techniques.

We find that, as predicted, the phenotype of the *Mgp*-tdTomato mouse was intensively red fluorescent in *Mgp*-expressing tissues. Paws and snout of the 2-week-old mice were visibly red (cartilage expression) and precluded genotyping. The enucleated eye exhibited red fluorescence in the same tissues that had been colored blue in our previous study[11] (TM and peripapillary sclera), recapitulating the specificity of *Mgp* expression in the eye. In addition, we showed for the first time that in vivo noninvasive fundus photography of the *Mgp*-tdTomato mouse exhibited a highly defined red fluorescent retinal vasculature, which then could be followed in a longitudinal manner. Relevant baseline biological and physiological parameters of the *Mgp*-tdTomato mice were shown to be no different than those of aged-matched wild-types (WTs). Therefore, the new *Mgp*-tdTomato mouse brings up a very useful tool to investigate longitudinally both mechanisms and therapeutics of glaucoma and angiogenesis diseases in the eye.

Methods

Mouse Strains

All animal work was performed as approved by the Institutional Animal Care and Use Committee at the University of North Carolina at Chapel Hill (UNC), and conducted in accordance with the ARVO Statement on the Use of Animals in Ophthalmic and Vision Research. All animals were housed in temperature-controlled rooms under standard 12-hour cycle lighting with food and water provided ad libitum.

The following three mouse strains were used in the study: (1) An $Mgp^{Cre.KI/Cre.KI}$ line that contains a knockin Matrix Gla (*Mgp*) gene fused to an internal ribosomal entry site and Cre recombinase coding sequences, generated in our laboratory.[11] (2) A Cre reporter mice (B6;129S6-$Gt(ROSA)26Sor^{tm9(CAG-tdTomato)Hze}$/J) (in the public domain, https://www.jax.org/strain/007905) harboring a *loxP*-flanked STOP cassette preventing transcription of a tandem dimer of a DsRed fluorescent protein variant (tdTomato)[15] (The Jackson Laboratory). The tdTomato is expressed when bred to mice that express Cre recombinase. The Rosa-CAG-LSL-tdTomato-WPRE targeting vector contains a CMV-IE enhancer/chicken beta-actin/rabbit beta-globin hybrid promoter (CAG), an *FRT* site, a *loxP*-flanked STOP cassette, the tdTomato sequence (two copies of the fluorescent protein), a woodchuck hepatitis virus posttranscriptional regulatory element (WPRE; to enhance the mRNA transcript stability), a polyA signal, and an *attB*/*attP*-flanked PGK-*FRT*-Neo-polyA cassette. The entire construct was inserted into the *Gt(ROSA)26Sor* gene locus between exons 1 and 2 (Ai9). (3) A C57BL/6J WT strain (stock # 000664; The Jackson Laboratory) for controls. The parental strains used in the study were in the C57BL/6J and B6;129S6 mixed genetic backgrounds, respectively.

Genotyping

Genotyping was performed using tail-tip DNA and PCR with four sets of primers (*Mgp* and *R26,* mutant and WT alleles) (Fig. 1). Tail DNA extraction and amplification were conducted using an AccuStart II GelTrack PCR SuperMix (2X) (#95136-100; Quanta Biosciences, Beverly, MA, USA) following the manufacturer's specifications. Briefly, a 2-mm piece of mouse tail was placed in 100 µL extraction buffer and incubated at 95°C for 30 minutes. The mixture was then cooled to room temperature (RT), 100 µL stabilization buffer added, and centrifuged. The supernatant was used as the DNA extract. For the PCR, 2.5 µL of the DNA extract was added to a mix containing 12.5 µL AccuStart II PCR SuperMix, 6 µL of 2 µM each of corresponding primers, and 4 µL nuclease-free water (total 25 µL). PCR amplification conditions for the *Mgp*-Cre.KI/WT alleles were 94°C 2 minutes (94°C 45 seconds, 58°C 40 seconds, 72°C 1 minute) for 40 cycles, and ending at 72°C for 2 minutes before holding the temperature at 4°C. For the *R26*-tdTomato/WT alleles, the cycle conditions were 95°C 30 seconds, 61°C 30 seconds, 72°C 30 seconds.

Primers designed to identify the *Mgp* alleles were from our publication.[11] For the WT allele (Mgp^{+}), the sequences of the primer pair were #1f 5′TGCCTACGAGATCAACAGAG3′ and #1r 5′ATGTGGTTACACCTCCACAC3′, which yields a 467-bp amplimer. For the mutant *Mgp*-Cre.KI allele, we used primers #2f 5′CTGGAGTTTCAATACCGGAG3′ and #2r 5′ATGTGGTTACACCTCCACAC3′, yielding a 690-bp amplimer. For the Rosa locus, primers were those recommended by The Jackson Laboratory (in the public domain, https://www2.jax.org/protocolsdb/f?p=116:5:0::NO:5:P5_MASTER_PROTOCOL_ID,P5_JRS_CODE:29436,007905). For the *R26*-WT allele, primers were #3f 5′AAGGGAGCTGCAGTGGAGTA3′ and #3r 5′CCGAAAATCTGTGGGAAGTC3′, which yields a 297-bp amplimer, and for the *R26*-tdTomato allele, the primers were #4f 5′CTGTTCCTGTACGGCATGG3′ and #4r 5′GGCATTAAAGCAGCGTATCC3′, which yields a 196-bp amplimer, as recommended.

Tissue Collection, Whole Mounts, and Histology

Mice were euthanized by CO_2 inhalation followed by cervical dislocation immediately before tissue collection. Whole globes were gently enucleated and imaged under a Leica MZ16FA fluorescence stereo microscope equipped with an Orca-ERG cooled monochrome charge-coupled device camera (Hamamatsu Photonics, Hamamatsu, Japan). For the anterior segment histology, whole globes were fixed in cold, freshly prepared 4% paraformaldehyde (PFA) in PBS for 1 hour with a slit a few millimeters posterior to the limbus. Anterior segments were then dissected and post fixed in the same medium at 4°C overnight. Next morning, tissues were immersed in 10% sucrose in PBS at 4°C for approximately 6 hours, transferred to 30% sucrose overnight, and embedded in optimum cutting temperature compound (Tissue-Tek; Sakura Finetek, Torrance, CA, USA). Cryoembedded blocks were sectioned meridionally at 10 µm, the sections stained with 4′,6-diamidino-2-phenylindole (DAPI), and mounted on glass slides at the UNC histology core facility (in the public domain, https://www.med.unc.edu/cellbiophysio/research-facilities/histology-facility). For the paraffin embedding, slit whole globes were fixed with 4% PFA for 24 hours, rinsed in deionized water for 10 minutes, immersed in 70% ethanol, and delivered to the UNC core for embedding (in the public domain, https://uncch.ilab.agilent.com/service_center/show_external/4429). Five-micrometer sections were either stained with hematoxylin-eosin (H&E) or processed for immunohistochemistry (IHC). After antigen retrieval, sections were cross-reacted with a rabbit anti-

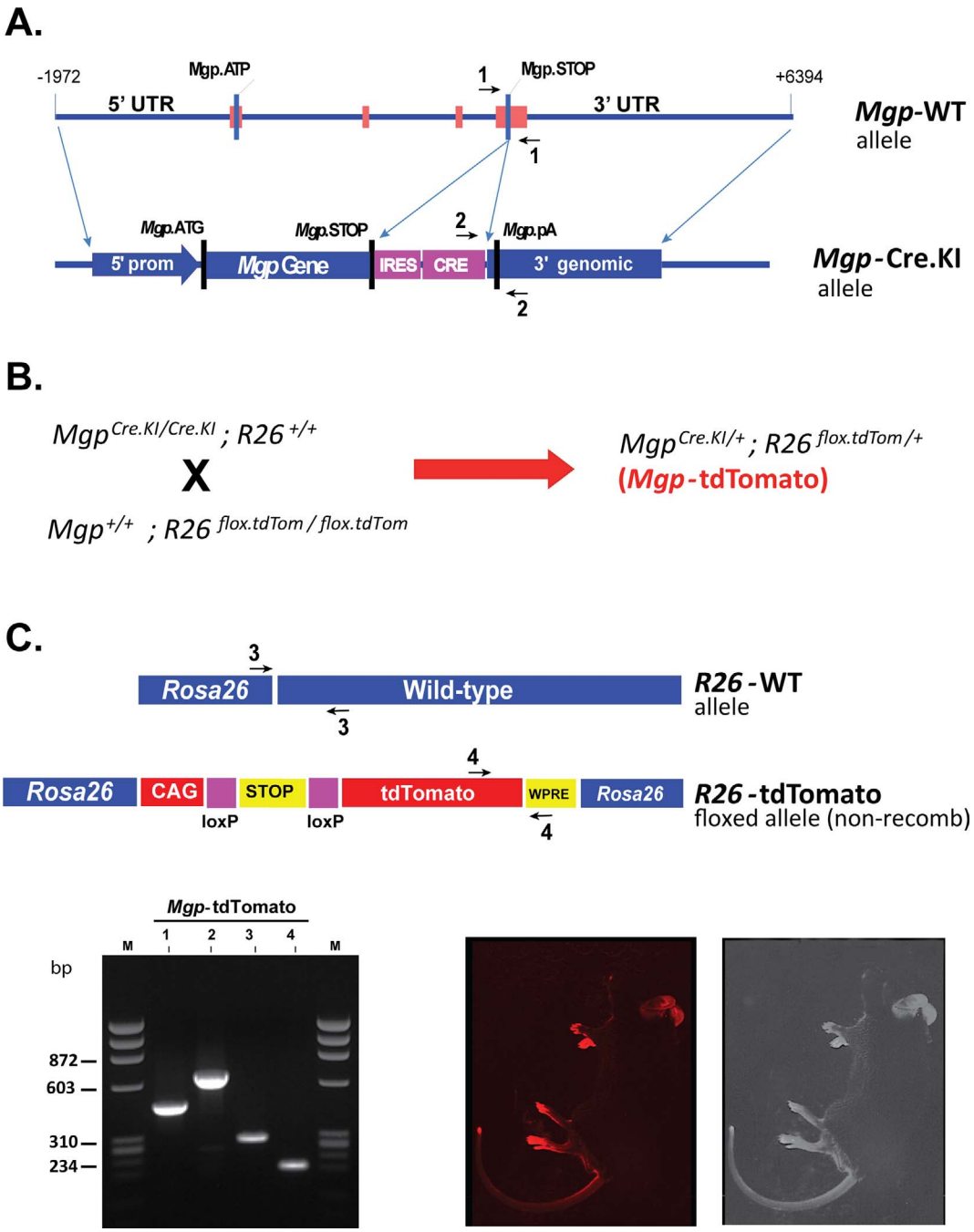

Figure 1. Generation and characterization of the *Mgp*-tdTomato transgenic mouse. (**A**) Diagram of the *Mgp*-WT and *Mgp*-Cre.KI alleles. The IRES-CRE elements in the *Mgp*-CRE.KI are inserted in exon 4, between the *Mgp* STOP and polyadenylation signals. (**B**) Diagram of the crossing of homozygous *Mgp*-Cre.KI mouse with homozygous *Rosa26* floxed tdTomato mouse. Double heterozygous containing both alleles (*Mgp*-tdTomato). The CRE recombinase driven by the *Mgp* elements floxes the tdTomato allele only in tissues where *Mgp* is expressed. (**C**) *Top*: Diagram of the *Rosa* locus WT and floxed tdTomato cassette alleles. The *arrowheads* denote the primer pairs used for each allele characterization. *Bottom left*: PCR performed with the indicated primer pairs on genomic DNA from the *Mgp*-tdTomato. *Bottom right*: Representative images of an *Mgp*-tdTomato mouse taken on a UV transilluminator. Phenotype shows fluorescent cartilage tissues.

Red Fluorescent Protein (anti-RFP) (catalog no. 600-401-379; Rockland Immunochemicals, Limerick, PA, USA) (1:500) overnight at 4°C, followed by incubation for 2 hours at RT with donkey anti-rabbit Alexa Fluor 594 (Thermo Fisher Scientific, Waltham, MA, USA) (1:2000). After PBS washes, slides were mounted with DAPI containing Fluoro-Gel II (Electron Microscopy Science, Hatfield, PA, USA). Images were taken on a model IX71 Olympus microscope equipped with a digital DP80 camera and cellSens software package (Olympus, Center Valley, PA, USA).

For visualization of the retinal vasculature, retinal flat mounts were prepared as described in our earlier publication[16] with a few modifications. Eyes were enucleated immediately after euthanization, and whole globes immersed in fresh 4% PFA with a corneal puncture overnight. Next morning, eyes were opened at the limbus with iridectomy scissors, lens and ciliary body removed, and retinal cups rinsed with PBS. Retinas

Investigative Ophthalmology & Visual Science

were separated from the underlying choroid/sclera while immersed in PBS using fine forceps, and released by sectioning the optic nerve. Retinas were then cleaned with craft brushes, and four clover radial cuts were made using a scalpel. Afterward, retinas were scooped and moved to Superfrost Plus slides (Thermo Fisher Scientific) with a Paton ophthalmic spatula (Wilson Ophthalmic, Mustang, OK, USA), flattened with the help of the brushes, and coverslipped with a drop of Fluoromount-G (Southern Biotech, Birmingham, AL, USA). Images were taken in an Olympus XI71 fluorescence microscope with a Texas Red Chroma filter of 560 nm excitation/bandwidth 55 nm and 645 nm emission/bandwidth 75 nm. The microscope was equipped with an Olympus DP70 digital camera and software. Digital images were arranged with Photoshop CS and Adobe Illustrator CS5 software (Adobe Systems, Inc., San Jose, CA, USA).

Live Intraocular Imaging (Fundus Photography)

Fundus imaging was conducted using the Micron IV retinal imaging microscope, with mouse objective and 50-degree field of view (1.8-mm diameter) (Phoenix Research Laboratories, Pleasanton, CA, USA). For direct fluorescence of the retinal and choroidal vasculatures, mice were anesthetized by intraperitoneal (IP) injection of a ketamine/xylazine/acepromazine cocktail (Butler Schein, Dublin, OH, USA) to achieve concentrations of 62.5 mg/kg (ketamine), 6.25 mg/kg (xylazine), and 1.25 mg/kg (acepromazine), respectively. Either before or after anesthesia, pupils were dilated by a drop of 1% tropicamide ophthalmic solution (Bausch & Lomb, Inc., Tampa, FL, USA), and allowed 2 to 5 minutes for complete dilation. A drop of Genteal lubricant gel (Alcon Laboratories, Fort Worth, TX, USA) was applied to the eyes to avoid cornea dehydration. Mice were then placed on the stage of the Micron IV with 3 degrees of rotation and the objective stereoscopically adjusted to come in contact with the cornea. To capture and image the tdTomato fluorescence (red) of the retina fundus, custom filters were purchased from Semrock, Inc. (Rochester, NY, USA) and installed at position 4 (see below).

For fluorescein angiography, approximately 5 minutes after anesthesia, mice were IP injected with 1% AK-FLUOR (Alcon) at the concentration of 100 µL per 20 g mouse. Immediately after, pupils were dilated, and mice placed on the Micron IV stage. Fluorescein-labeled images were acquired using a filter with excitation of 486 nm and emission of 536 nm (green).[17–19] All retina fundus images were obtained using the StreamPix Software (Phoenix Research Laboratories, Pleasanton, CA, USA) and adjusted to include the optic nerve.

Laser-Induced Choroidal Neovascularization (CNV)

Laser-burn photocoagulations were induced following standard protocols.[17,20] For this, mice were anesthetized, pupils dilated as indicated above, and taken to the Micron IV stage. The laser burns were induced under the red fluorescence filter to visualize the retinal vasculature (guided image). Three laser burns (each 532 nm, 440 mW, 80 ms) were applied to each eye. Locations were chosen surrounding the optic nerve (approximately 10, 2, and 4 o'clock positions) and in-between the retinal vessels. After acquiring bright field images, mice were IP injected with fluorescein while at the stage, followed by subsequent acquisition of sequential images in the green and red channels. Images taken immediately after laser (day 0) were also retaken at days 3, 6, and 14 after the induced injury following fresh fluorescein injections. A prelaser set of images was also taken 10 days before the laser application. After imaging, topical ophthalmic antibiotic ointment (neomycin 3.5 mg/g, polymyxin B 10,000 U/g, and bacitracin 400 U/g; Akorn, Lake Forest, IL, USA) was placed on the eyes of the mice. Animals were then laid on a 37°C warm bed until fully awake before returning to the housing facility.

Measurement of IOP

IOPs were measured unmasked on sedated mice, using a calibrated TonoLab selected for mouse settings (Colonial Medical Supply, Franconia, NH, USA) and equipped with foot pedal. The mice were lightly anesthetized with the same ketamine/xylazine/acepromazine cocktail but to achieve lower concentrations of 41.7 mg/kg (ketamine), 4.2 mg/kg (xylazine), and 0.83 mg/kg (acepromazine), respectively. At this anesthesia concentration, mice achieve recumbency in 3 to 5 minutes. An eye drop of 0.5% tetracaine (Bausch & Lomb) was applied before the measurements. All IOP measurements were conducted following the manufacturer's recommendations. Only mean values with an SD (expressed as percentage of the mean) less than 5% were accepted. All IOP measurements were taken between 1:00 and 3:00 PM, at 3 minutes after recumbency. Data were analyzed using the SigmaPlot software (Systat Software, Inc., San Jose, CA, USA) and are presented as means ± SEM.

Electroretinograms

Full-field ERG analyses were performed as previously described.[17,19,21,22] In brief, after overnight dark adaptation, mice were anesthetized by IP injection of 62.5 mg/kg ketamine, 6.25 mg/kg xylazine, and 1.25 mg/kg acepromazine (Butler Schein) in the dark and their eyes subsequently dilated with 1% tropicamide (Bausch & Lomb). Each mouse was placed on a 37°C platform throughout the full-field ERG recordings. The scotopic response was assessed with a stimulus intensity of 4 log cd s/m^2 to the dark-adapted eyes in an Espion E^2 electroretinography system (Diagnosys LLC, Lowell, MA, USA). The amplitude of the scotopic a-wave, generated primarily by photoreceptor cells, was measured from the prestimulus baseline, to the a-wave trough. The amplitude of the scotopic b-wave was measured from the trough of the a-wave, to the crest of the b-wave. To evaluate photopic response, animals were light adapted for 5 minutes under a light source of 30 log cd s/m^2 to bleach the rod-mediated responses. Afterward, a strobe flash was presented to the eyes with a stimulus intensity of 2.25 cd s/m^2. The amplitude of the photopic b-wave was measured from the trough of the a-wave, to the crest of the b-wave.

Statistical Analysis

Average values are expressed as means ± SE. The significance of experimental changes was analyzed using Student's *t*-test as unpaired data using SigmaPlot software (Systat). For the calculation of *P* values, all technical replicates from all biological replicates were used. A value of 0.05 was chosen as the level of significance. The power of the experiments was determined using the GraphPad StatMate2 software (GraphPad Software, Inc., La Jolla, CA, USA).

Results

Generation of the *Mgp*-tdTomato Transgenic Mouse

We had previously generated an *Mgp*-Cre.KI mouse in which the mouse *Mgp* gene was fused to an internal ribosomal entry site (IRES)-Cre recombinase cassette and knocked-in to a

C57BL/6J mouse.[11] In this mouse, the Cre cassette was inserted between the 5′ and 3′ arms of the *Mgp* gene, and 3′ to the *Mgp* STOP to ensure expression of the functional protein in the corresponding tissues (Fig. 1A).

For the creation of an *Mgp*-tdTomato mice, we crossed our *Mgp*-Cre.KI mouse[11] with the *R26*-tdTomato reporter.[15] Males and females from both strains were crossed indistinctively to generate an F1 of double-heterozygous $Mgp^{Cre.KI/+}$; $R26^{flox.tdTom/+}$ mice (*Mgp*-tdTomato) (Fig. 1B). The life span, weight, fertility, and litter size (six to nine pups per litter) of this F1 were no different from those of WT. Genotyping of the *Mgp*-tdTomato mouse with primer pairs showed the correct amplimer's size for the four alleles: 469 bp (*Mgp* WT), 690 bp (*Mgp* mutant), 297 bp (*R26* WT), and 196 bp (*R26* mutant) (Fig. 1C, lower left). To date, we have examined and confirmed genotyping of more than 50 experimental mice, ages ranging from 1 to 5 months and from different founders. Because the *Mgp* gene is also known to be highly expressed in cartilage,[23] these mice exhibited red color paws, tail, and snout, which are distinguishable by direct observation, but highly noticed when placed on top of a UV transilluminator source (Fig. 1C, lower right). This marked, innocuous phenotype is seen clearly in 2- to 3-week-old pups and provides an easy identification marker for the *Mgp*-tdTomato mice. This phenotype further validates the functional activity of the Cre recombinase of the *Mgp*-Cre.KI mouse in systemic tissues where *Mgp* is known to be expressed. Although a double-homozygous $Mgp^{Cre.KI/Cre.KI}$; $R26^{flox.tdTom/flox.tdTom}$ could not be generated due to leakage of *Mgp* expression in the germ line, the F1 double-heterozygous provided strong fluorescent intensity for all applications tried. In addition, the red paws/snout phenotype precluded the need for genotyping.

Fluorescence of the Enucleated Eye and TM Histology

Mgp-tdTomato freshly enucleated eye globes frontally placed under a dissecting fluorescence stereo microscope and facing the microscope lens showed a strong red fluorescent circle at the limbus area (Fig. 2A). Rotation of the globe allowed better determination of the fluorescence location at the limbus area and further revealed an intense fluorescence in a small button-like region at the optic nerve head (Figs. 2B, 2C). The pattern was the same in all eyes examined and in litters from the two original founders.[11] Images were taken on six representative mice (both eyes) from three different litters. Breeding pairs for the litters were set up with crosses of both a female *Mgp*-Cre.KI mouse with a male *R26*-tdTomato and a male *Mgp*-Cre.KI with a female *R26*-tdTomato. Age of the imaged *Mgp*-tdTomato mice spanned from 1 month to 2.5 months.

To assess the underneath location of the fluorescent circle observed on the whole globe, anterior segments were fixed overnight, cryoembedded, and processed for histologic evaluation. Meridional sections of the angle area exhibited a natural intense red fluorescence in the outflow pathway region including all cell layers of the TM and extending to the ciliary muscle (Figs. 2D, 2E). Staining of cryo-sections with DAPI clearly identified the Schlemm's canal (SC) (Fig. 2F). An additional four eyes were paraffin-embedded after fixing, and processed for H&E morphology and IHC with an anti-RFP antibody. Meridional 5-μm H&E sections showed a well-developed TM and SC (Figs. 2G, 2H). The antigen retrieval IHC showed an intense immunofluorescence at the same site observed by the direct fluorescence of the protein (Fig. 2I). Adjacent sections cross-reacted only when the secondary antibody showed no fluorescence at the same conditions (not shown). The localization of the *Mgp* Cre-mediated expression either visualized directly or by IHC, was nearly identical in all mice analyzed.

Other than the retinal flat-mount staining, not done on the *Mgp-LacZ* mouse, the fluorescent pattern of *Mgp*-tdTomato mice observed here fully corresponded with the histologic pattern obtained with the *Mgp-LacZ* mouse.[11] Thus, these results recapitulate and validate the spatial expression of the *Mgp* gene in the eye and place this gene and this mouse as a desirable marker for future studies.

Retinal and Choroidal Vasculatures of the *Mgp*-tdTomato Mouse Are Naturally Fluorescent

The *MGP* gene is known to be highly expressed in the VSMC of arteries[3,24] and an *Mgp*.KO mouse dies at 4 to 5 weeks of age due to massive arterial calcification.[12] To investigative whether the VSMC of the mouse retinal vessel wall expressed the *Mgp* gene, and whether these vessels would be fluorescent in the *Mgp*-tdTomato mouse, we first performed histologic assessments in flat mounts.

Retinal flat mounts were prepared from both eyes of five 2- to 3-month-old mice. After overnight fixation and post-dissection, all arteries and capillaries of the retina were highly fluorescent red. The overall retinal vasculature was nicely visible, sharp, and very well defined. A great number of bright red capillaries were observed branching from the main retinal arteries (Figs. 3A, 3B). To determine whether the choroidal vasculature was also fluorescent, despite the lower number of VSMCs in their vessels,[25] we prepared a choroidal whole mount. We observed a characteristic pattern of choroidal vasculature whole mounts, with vessels appearing as circular openings surrounded by a fluorescent vessel wall (Figs. 3C, 3D). As expected, fluorescence intensity of the choroid vasculature in the whole mount was lower than the one in the retina. This was due not only to the diminished number of VSMC layers in the choroidal vessels, but to their different orientation in this type of preparation. Both these results opened the door to the opportunity of studying eye vascular diseases in this new mouse model without the need of administering fluorescein to visualize the vessels.

Imaging of the *Mgp*-tdTomato Mouse Retinal Vasculature in Living Animals

To directly assess the fluorescent vasculature in vivo, we used the Micron IV retinal imaging microscope (Phoenix). To acquire the tdTomato fluorescence, we tested several filters. We found that an exciter, single-band bandpass filter 554 nm with a bandwidth of 23 nm together with an emitter (barrier) single-band 609 nm with a bandwidth of 54 nm gave the best results. The size of the exciter was 25 mm in diameter and it was commercially available. The diameter of the barrier was 12.5 mm, and it was custom made (Semrock, Inc.).

Figure 4 shows fluorescent retinal vasculatures of six random mouse eyes, 2 to 3 months old. In all of them, the retinal vasculature could be easily imaged. The fluorescence intensity does not appear to vary with age and extends to the capillary bed, an indication that *Mgp* is also naturally expressed in the pericytes.[26] When one of the mice was IP injected with fluorescein, the image of the vasculature in the green channel overlapped with the red fluorescence of the cells expressing *Mgp* (Fig. 4, mouse 6). These results bring up the relevance of a fluorescent animal model that exhibits high specificity for the retinal vascular bed. Furthermore, the expression of the Cre recombinase responsible for the red fluorescence is under the control of the entire *Mgp* regulatory regions. This, plus the abundant expression of this gene, makes our *Mgp*-tdTomato mice a model with a tighter and stronger specificity than other

Investigative Ophthalmology & Visual Science

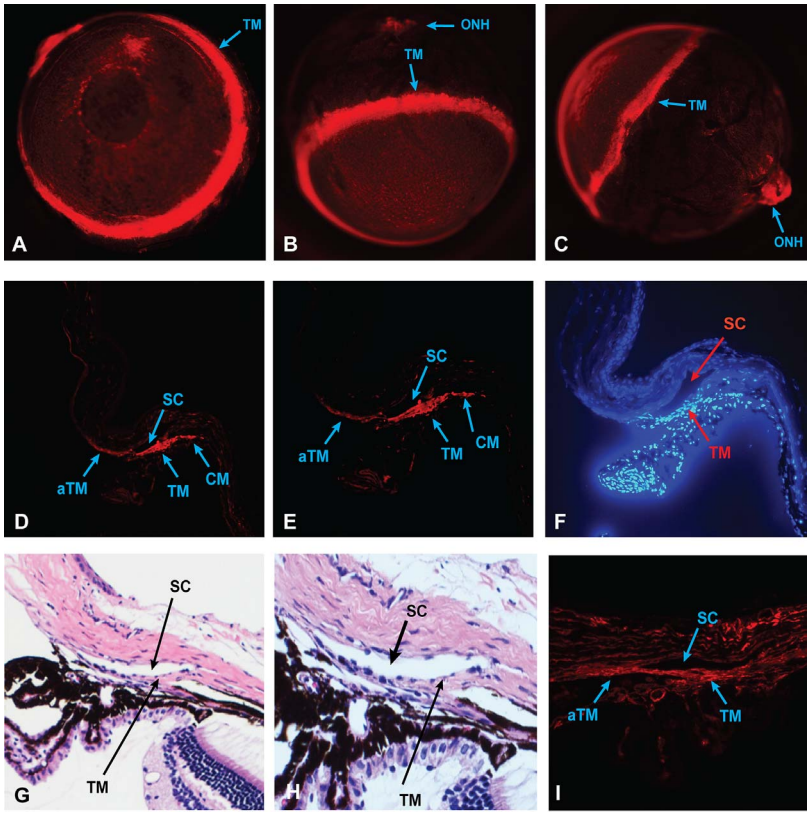

Figure 2. Direct fluorescence, morphology, and IHC of the *Mgp*-tdTomato mouse's anterior segment. *Top row*: Representative images of an enucleated whole globe captured under a fluorescence dissecting stereo microscope. (**A**–**C**) Frontal and rotating side views showing an intense fluorescence circle at the limbus and a confined small region at the optic nerve head (ONH). Original magnification, ×170 (**A**) and ×160 (**B**, **C**). *Middle row*: Histologic assessment of the mouse eye angle area. Representative frozen meridional sections, 10-µm thick, showing specific fluorescence in the outflow region extending to the ciliary muscle. (**D**, **E**) Direct fluorescence; (**F**) DAPI staining. *Bottom row*: Representative paraffin-embedded 5-µm sections stained with H&E (**G**, **H**) and cross-reacted with a rabbit anti-RFP primary and Alexa Fluor 594 donkey anti-rabbit secondary antibodies (**I**). Detection of expression of *Mgp*-tdTomato by direct fluorescence overlaps that seen by IHC. TM, trabecular meshwork; aTM, anterior TM; CM, ciliary muscle; SC, Schlemm's canal. Original magnification, ×100 (**D**), ×200 (**E**–**G**, **I**), ×400 (**H**).

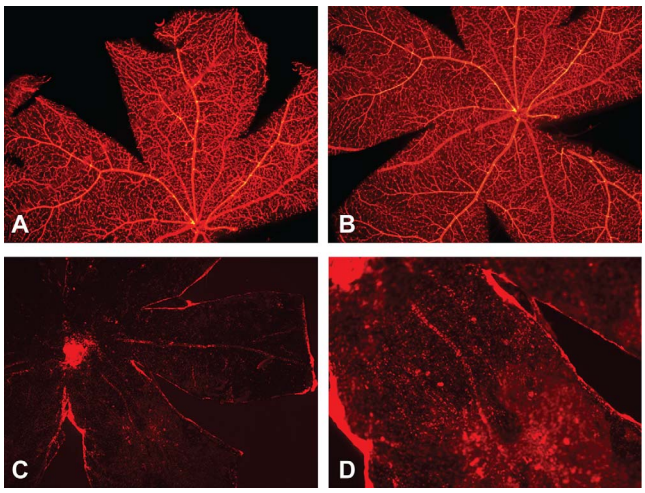

Figure 3. Natural fluorescence of the *Mgp*-tdTomato mouse retinal and choroidal vasculatures. (**A**, **B**) Two field views of a representative image from a single retinal flat mount of a 2.5-month-old *Mgp*-tdTomato mouse. Original magnification, ×40. (**C**, **D**) Representative image from a single choroidal whole mount of a 1.5-month-old *Mgp*-tdTomato mouse. Original magnification, ×40 (**C**); ×100 (**D**). The natural red fluorescence is well defined and thoroughly extends to the capillary bed.

transgenic animals carrying a limited promoter fused to a fluorescent protein.

Laser-Induced CNV in the *Mgp*-tdTomato Mouse

CNV is a hallmark of wet-AMD; 10% to 20% of AMD cases belong to this (wet form) irreversible condition. To elucidate wet-AMD mechanisms and to search for therapeutics to treat the disease, the laser-induced CNV model is the most popular one. It entails the use of laser to guide choroidal insults at the Bruch's membrane, which results in both leakiness and proliferation of the choroidal vascular bed. Current evaluation of this model is conducted by IP injection of fluorescein, which flows through the circulatory system and allows assessing both parameters by noninvasive living imaging. As a proof of concept for the utilization of the *Mgp*-tdTomato mouse for angiogenesis-affected eye diseases, we induced laser burns in the eyes ($n = 18$) of 2.5-month-old male and female mice. We first found that the guided application of three laser burns was greatly facilitated by the presence of naturally red fluorescent vessels and that the effects of the burns could be followed longitudinally in a noninvasive manner. For a more specific determination of the correlation of the fluorescein circulating dye marker with that of the cells of the vessel wall, we performed a longitudinal time-point experiment for 2 weeks ($n = 4$ mice, 8 eyes). Images of one representative eye are shown in Figure 5. At every time point, fluorescein was injected after

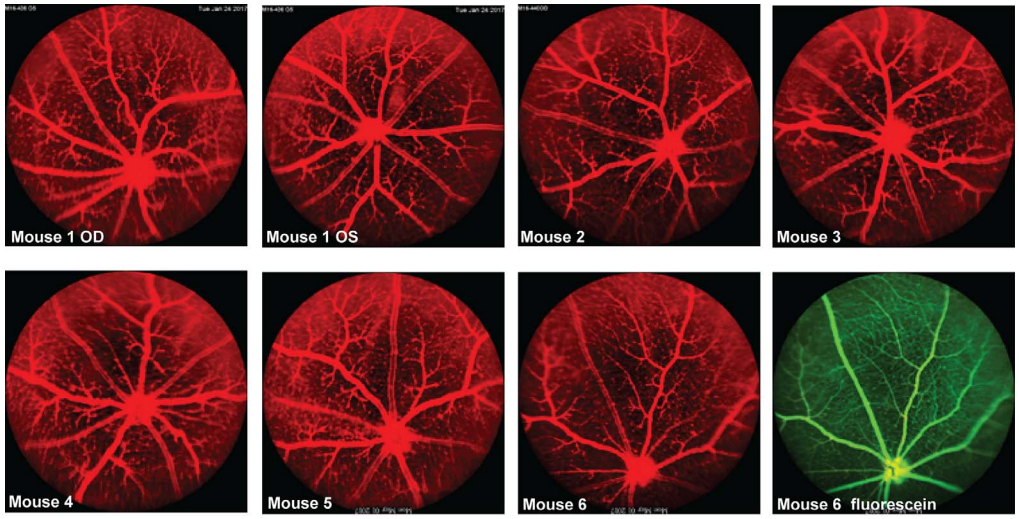

Figure 4. Noninvasive fundus imaging of the living *Mgp*-tdTomato mouse. Representative images from a set of six *Mgp*-tdTomato mice, ages 2 to 3 months old. Images were captured from either both eyes (mouse 1) or a single eye (mice 2 to 6). Mouse 6 fluorescein: injected IP with fluorescein. Images were obtained in a Micron IV retinal imaging microscope with a 25-mm 554/23 nm excitation, and a 12.5-mm 609/54 nm emission filter. Natural fundus fluorescence of the *Mgp*-tdTomato mouse matches that of the injected fluorescein. Labeling of the retinal vasculature in the *Mgp*-tdTomato mouse is permanent, and can be followed longitudinally.

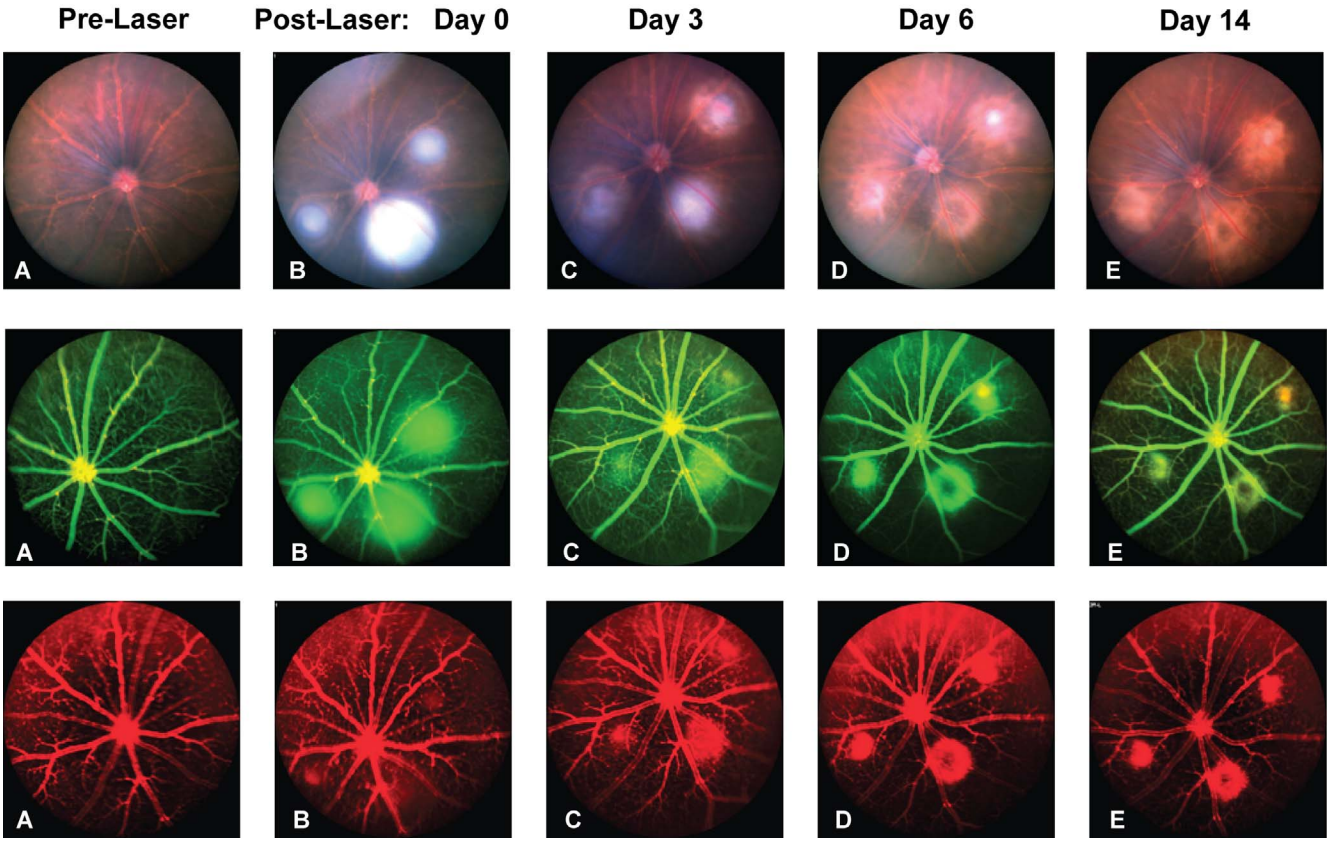

Figure 5. Separation of CNV's leakiness and neovascularization outcomes in the *Mgp*-tdTomato mouse. Representative laser-induced photocoagulation burns induced at day 0 and followed for 3, 6, and 14 days ($n = 18$ eyes). Fundus images from the same eye of a single mouse were captured in a Micron IV retinal imaging microscope. Pictures were taken at 10 days prelaser (**A**), and postlaser injury day 0 (**B**), day 3 (**C**), day 6 (**D**), and day 14 (**E**). At each time point, mice were set at the stage and pictures acquired in bright field (*top*). Immediately after, while in the stage, mice were injected IP with fluorescein followed by acquisition of additional pictures in the green (*middle*) and red (*bottom*) channels. Vessel leakiness was observed in the green channel (fluorescein). Neovascularization was observed in the red channel due to vessel wall fluorescence of the *Mgp*-tdTomato mouse.

Investigative Ophthalmology & Visual Science

the bright field image acquisition and immediately followed by sequential images in the green and red channels. Images taken 10 days before the laser injury showed a comparable vessel definition of the temporary (green) and the resident (red) markers (Fig. 5A). Right after the laser burns (day 0), we observed well-defined green spots indicating rapid leakage of the capillaries. Not matching red spots were observed on the red channel at the same time (Fig. 5B). This was because the red florescence in the *Mgp*-tdTomato mouse comes from the VSMC forming the vessel wall and not from the vascular flow of a fluorescent dye. At 3 days, the green spots began to weaken, and matching red spots began to appear in the red channel, indicating vascular proliferation at the site of the burns (Fig. 5C). The vascular proliferation spots continued to further develop at day 6 and appeared to begin receding at day 14, when the experiment was terminated (Figs. 5D, 5E). In parallel, leakage determined by the green spots continued to subside. The same results were observed in all eyes of the group. Whether the red spots on days 3 to 14 were due to vessel proliferation or to recruitment of pericytes cannot be distinguished at this time (see discussion below).

Altogether, these results showed that, in contrast to the use of fluorescein, which cannot distinguish between leakage and proliferation, the *Mgp*-tdTomato mouse provides the option of assessing vessel proliferation independently. This new transgenic model involving a well-characterized VSMC gene would provide an important tool for the more accurate assessment of angiogenesis therapeutics.

Physiological Characterization of the *Mgp*-tdTomato Mouse

To assess whether expression of the fluorescent protein had affected relevant physiological parameters for the study of glaucoma and angiogenesis in the *Mgp*-tdTomato mice, we measured their IOP and retinal function (ERG) and compared them with those of age-matched control WT mice (Fig. 6).

Intraocular Pressure. IOPs were measured in both eyes of two groups of 2.8-month-old mice (*Mgp*-tdTomato and WT controls) ($n = 10$ eyes for the *Mgp*-tdTomato mouse and $n = 8$ eyes for the WT). All but one of the total nine mice were male. For each mouse, IOPs were taken in both eyes once a week for 3 consecutive weeks. All IOP values of each group were pooled and compared ($n = 30$ measurements for the *Mgp*-tdTomato mice and $n = 24$ measurements for the WT). The mean IOP of the *Mgp*-tdTomato group was 9.2 ± 0.35 mm Hg, and that of the WT group was 8.7 ± 0.22 mm Hg. The IOP of the *Mgp*-tdTomato mice was not significantly different than that of the WT group ($P = 0.275$) (Fig. 6A).

Electroretinography. Full-field ERGs were evaluated with age-matched (3- to 4-month-old) *Mgp*-tdTomato ($n = 6$ eyes) and WT controls ($n = 6$ eyes) (Fig. 6B). The a-wave and b-wave responses were observed in both eyes of each mouse under scotopic and photopic settings. Both the scotopic and photopic ERG responses from *Mgp*-tdTomato and WT mice were collected and analyzed. The mean of photopic a-waves of *Mgp*-tdTomato and WT groups were 31.8 ± 4.9 μV and 50.5 ± 15.1 μV, respectively ($P = 0.268$). The photopic b-waves of *Mgp*-tdTomato and WT mice had amplitudes of 146.3 ± 17.1 μV and 136.8 ± 30.5 μV, respectively ($P = 0.791$). For the dark-adapted scotopic, a-waves of *Mgp*-tdTomato and WT showed 54.0 ± 8.2 μV and 64.0 ± 11.6 μV ($P = 0.499$), whereas scotopic b-waves exhibited 177.0 ± 22.2 and 174.0 ± 32.1 μV amplitudes, respectively ($P = 0.940$). Altogether, these results demonstrated that photopic and scotopic ERG responses of *Mgp*-tdTomato and WT mice were not significantly different. Therefore, these promising outcomes support that the retinal function of *Mgp*-tdTomato mice is comparable to that of WT control.

Discussion

In this study, we reported the generation of a new transgenic fluorescent mouse model for the longitudinal study of glaucoma and angiogenesis.

In glaucoma, physiological and pharmacologic in vivo studies have been hampered by the inability to follow the effects of treatment(s) on relevant tissues longitudinally. Such limitations precluded investigating whether insults, drugs, and/or age would have a pathologic damaging effect, cell death, and/or induce a proliferative effect on the glaucoma tissues over time. The new *Mgp*-tdTomato model presented here overrides such limitations. The glaucoma tissue–specific fluorescence is sufficiently strong to be followed by available noninvasive imaging techniques for the life of the animal.

In addition to studying effects of external inducers, a fluorescently labeled TM could provide a way to investigate numerous biological properties of the tissue. It would allow, for instance, to revisit established paradigms, such as the loss of TM cells with age,[27,28] or segmental flow,[29–31] and determine the cellularity of flow and nonflow regions. Likewise, a labeled TM will be of great use for stem cell research. Stem cells from the TM of an *Mgp*-tdTomato mouse could be isolated by fluorescence-activated cell sorting before transplantation into a new recipient mouse. Assessing homing and repopulation of the TM tissue in new animals would be much easier because the incoming TM stem cells would be fluorescently labeled.

Studies on the retinal/choroidal vasculature are of utmost importance for the eye. In glaucoma, vascular health, including arterial stiffness, has been proposed to be one of the elevated IOP alternative risk factors for the disease.[32,33] Vascular etiology has been postulated as playing a role in the development of normal-tension glaucoma and the possible explanation as to why some patients' glaucoma progresses in the presence of reduced IOP, whereas that of others with elevated IOP do not develop glaucoma.[33] A correlation has also been known to exist between the higher incidence of glaucoma in individuals of African descent and their elevated high incidence of cardiovascular diseases.[34] Thus, a mouse model with a fluorescent eye vasculature could be very useful to study the structural differences of the retinal vascular bed under glaucomatous conditions and to investigate the vascular theory of glaucoma.

A naturally fluorescent vasculature also would be very valuable for angiogenesis studies. The neovascular or wet form of AMD is characterized by the invasion of abnormal choroidal and retinal blood vessels and by their leakage into the retina. Vascular proliferation and vessel leakiness are the two major outcomes currently used to investigate causative factors of the disease, as well as being hallmarks for drug screening. To date, labeling of the vessels for such studies is conducted by injecting systemically a fluorescent dye (fluorescein), whose residence time in the circulation is very short.[35] Fundus photography immediately after the injection allows visualization of the vascular network at one given time point. An important advantage of our new transgenic mouse model is that, instead, the fluorescence in the vascular cells is permanent, thus allowing investigation of changes in the vascular network longitudinally and for the life of the animal. In addition, the physiological characteristics of the *Mgp*-tdTomato mouse, IOP and ERG, are not different from those of age-matched WT controls, which further validates them for

Investigative Ophthalmology & Visual Science

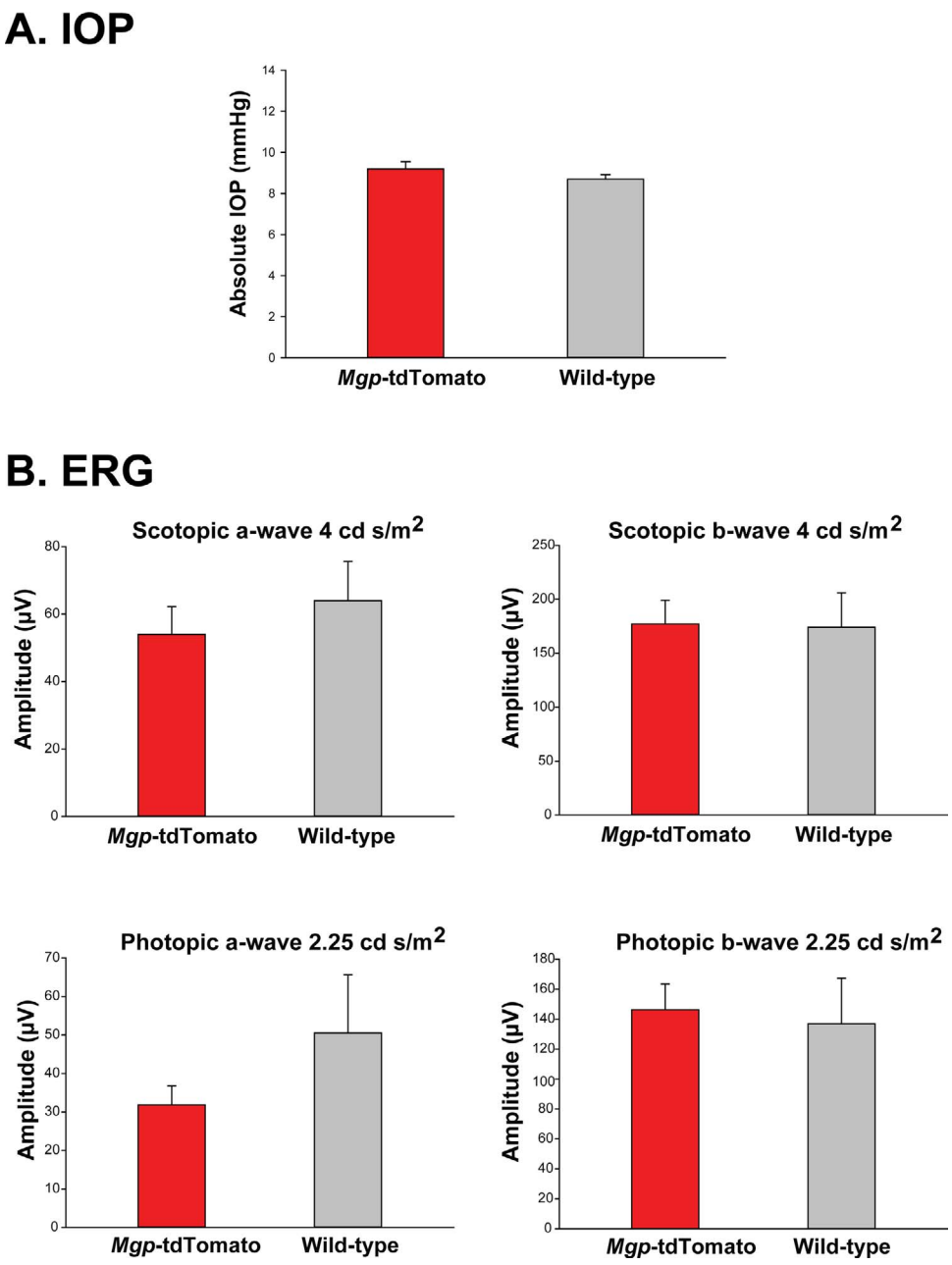

Figure 6. Physiological parameters of the *Mgp*-tdTomato mouse. (**A**) IOP was measured in 2.8-month-old mice once a week for 3 weeks. *Mgp*-tdTomato, $n = 10$ eyes, 30 measurements; WT, $n = 8$ eyes, 24 measurements. The mean IOP of the *Mgp*-tdTomato group was not significantly different from that of the WT group ($P = 0.275$). (**B**) Full-field ERG was performed in 3.5-month-old mice. *Mgp*-tdTomato and WT ($n = 6$ eyes each group). The a- and b-wave responses under scotopic (*top*) and photopic (*bottom*) settings from the two groups were not significantly different (scotopic: a-wave $P = 0.49$; b-wave $P = 0.94$; photopic: a-wave $P = 0.27$; b-wave $P = 0.79$). TM and retinal function outcomes of *Mgp*-tdTomato are undistinguishable from those of the healthy controls.

their use to appropriately assess glaucoma and retina outcomes.

As a proof of concept, in this study, we used the laser-induced CNV model[20] in the *Mgp*-tdTomato mouse and evaluated the retinal vasculature outcomes. We found that the detail and intensity of the naturally fluorescent vascular network (red channel) was very high, comparable to, if not better than, the one seen from the circulating fluorescein (green channel). Immediately after the laser burn, localized laser-injured spots were seen in the green but not in the red channel, whereas spots in the red channel appeared at the same location after 3 days. We interpret this finding as to say that there was an instant leakage response of the laser-injured vessels, which was detected by the extravasation of the circulating dye, whereas no additional wall-labeled vessels were detected at the same time. The sequence of appearance of the fluorescent spots after induction of the laser burns revealed that although the fluorescein injection method is unique to detect vessel leakiness, it cannot discern between vessel leakiness and neovascularization. The fluorescent red spots in the *Mgp*-tdTomato mouse will serve, instead, to evaluate just vessel proliferation. The ability of distinguishing between the two outcomes after injury could prove to be very valuable when screening drugs for AMD therapeutics. At this

time though, we do not know whether the red fluorescent spots observed are just the result of the formation of new blood vessels or whether they are perhaps due to the recruitment of pericytes. MGP has been showed to be expressed in pericytes and to be involved in the regulation of their differentiation and calcification.[26]

A considerable number of fluorescent transgenic mouse models with labeled neuroretina and RPE cellular layers are available. In contrast, very few of these models provided a fluorescent vascular retina.[36,37] In those mice, the promoter of a gene known to be expressed, albeit not specifically, in the vascular cells is driving a fluorescent reporter protein. Using a promoter to control expression of the reporter has the advantage of being able to turn on and off the gene and, as a consequence, the labeling of the targeted cell. In turn, however, the promoter approach has the disadvantage of the limited presence, often neither complete nor well-determined, of tissue-specific regulatory regions. The intensity of the fluorescence is also often lower for the same reasons. The Cre.KI-*loxP* mouse approach presented here determines the true expression of the gene. The Cre enzyme is inserted after the *Mgp* STOP signal and it is under the control of an entire, undisturbed *Mgp* gene (Fig. 1A). In this approach, though, once the fluorescent reporter allele is floxed (when the gene is first expressed), the labeling of the cell is permanent. That is, from then on, the fluorescence in that particular cell would disappear only when the cell is damaged or dead. By the same principle, the fluorescence would be expanded and reappear when new cells expressing *Mgp* are generated, such as occurs in the case of angiogenesis. This property could be an advantage or disadvantage, depending on the type of study. Overall, both types of transgenic fluorescent mechanisms would prove very useful in different applications.

Recently, an approach using a nano-lantern reporter knocked-in after exon 1 of the fetal liver kinase 1 (*FLK1*) gene has been published.[38] This new approach combining the KI technology with a dual fluorescence/bioluminescence reporter could be very powerful. It would allow study of gene regulation of a non-phototoxic reporter under the control of all and mostly undisturbed regulatory sequences. Because the flk1 gene (a VEGF receptor) is expressed in the vascular endothelial cells, the model also will serve for the study of angiogenesis. For all these approaches, the choice of the right gene is critical. One important advantage of the *Mgp*-tdTomato model presented here lies on the previous characterization of the *Mgp* in the eye, and on the finding of its unique specific expression in anterior and posterior segment tissues that are involved in glaucoma.[11] The long and well-recognized history of the MGP protein's relevance on the vascular system[9,12,39] uncovered the retina vasculature visualization shown here and provided a unique opportunity to study an interaction of all parameters simultaneously in the same mouse, and longitudinally. An added bonus to our approach is the simplicity of generating the same mouse with different fluorophores. In other words, crossing the *Mgp*-Cre.KI with the floxed collection of reporter mice available[40] (The Jackson Laboratory) will generate F1 mice that would have the same tissues described here fluorescent but in a different color. Using the correct filters on the eye live imaging microscopy, this property would open the door to experiments that would benefit for combining more than one fluorophore.

In summary, we report a new fluorescent marker mouse for the combined and/or independent studies of glaucoma and angiogenesis. Although there are quite a few reports for the use of fluorescence transgenic lines for systemic studies,[41] only a handful exist for the eye, and none is available for the tissues reported here. To our knowledge, this is the first model to observe specifically fluorescent TM and peripapillary sclera, plus the first one to combine in one animal their fluorescence with that of the retinal vasculature. The strategy used to generate this mouse further allows for one-step generation of mice with different fluorophores. Thus, the noninvasive longitudinal assessment of relevant tissue changes in the *Mgp* fluorescent mouse opens a new avenue for the investigation of both mechanistic and translational applications. Albeit the limitation of the same-cell temporal induction, the *Mgp*-tdTomato mouse provides a unique tool for the understanding of the integration of anterior-posterior segment glaucomatous responses in conjunction with the vascular system. The *Mgp*-tdTomato mouse also provides a unique tool for assessment of pharmaceuticals targeting the neovascularization effects of AMD.

Acknowledgments

The authors thank Ellen R. Weiss for allowing generous access to her ERG instrumentation, and to Laura Rodriguez Estevez for critical reading of the manuscript.

Supported by National Eye Institute Grants EY026220 (TB), EY11906 (TB), EY024059 (ZH), and EY026564 (ZH).

Disclosure: **P. Asokan**, None; **R.N. Mitra**, None; **R. Periasamy**, None; **Z. Han**, None; **T. Borrás**, None

References

1. Luo G, D'Souza R, Hogue D, Karsenty G. The matrix Gla protein gene is a marker of the chondrogenesis cell lineage during mouse development. *J Bone Miner Res*. 1995;10:325–334.
2. Shanahan CM, Weissberg PL, Metcalfe JC. Isolation of gene markers of differentiated and proliferating vascular smooth muscle cells. *Circ Res*. 1993;73:193–204.
3. Wallin R, Wajih N, Greenwood GT, Sane DC. Arterial calcification: a review of mechanisms, animal models, and the prospects for therapy. *Med Res Rev*. 2001;21:274–301.
4. Gonzalez P, Epstein DL, Borrás T. Characterization of gene expression in human trabecular meshwork using single-pass sequencing of 1060 clones. *Invest Ophthalmol Vis Sci*. 2000; 41:3678–3693.
5. Vittitow J, Borrás T. Genes expressed in the human trabecular meshwork during pressure-induced homeostatic response. *J Cell Physiol*. 2004;201:126–137.
6. Gonzalez P, Epstein DL, Borrás T. Genes upregulated in the human trabecular meshwork in response to elevated intraocular pressure. *Invest Ophthalmol Vis Sci*. 2000;41:352–361.
7. Comes N, Borrás T. Individual molecular response to elevated intraocular pressure in perfused postmortem human eyes. *Physiol Genomics*. 2009;38:205–225.
8. Xue W, Comes N, Borrás T. Presence of an established calcification marker in trabecular meshwork tissue of glaucoma donors. *Invest Ophthalmol Vis Sci*. 2007;48:3184–3194.
9. Borrás T. A single gene connects stiffness in glaucoma and the vascular system. *Exp Eye Res*. 2017;158:13–22.
10. Du Y, Yun H, Yang E, Schuman JS. Stem cells from trabecular meshwork home to TM tissue in vivo. *Invest Ophthalmol Vis Sci*. 2013;54:1450–1459.
11. Borrás T, Smith MH, Buie LK. A novel Mgp-Cre knock-in mouse reveals an anticalcification/antistiffness candidate gene in the trabecular meshwork and peripapillary scleral region. *Invest Ophthalmol Vis Sci*. 2015;56:2203–2214.
12. Luo G, Ducy P, McKee MD, et al. Spontaneous calcification of arteries and cartilage in mice lacking matrix GLA protein. *Nature*. 1997;386:78–81.

13. Boström K, Zebboudj AF, Yao Y, Lin TS, Torres A. Matrix GLA protein stimulates VEGF expression through increased transforming growth factor-beta1 activity in endothelial cells. *J Biol Chem*. 2004;279:52904–52913.
14. Xue W, Wallin R, Olmsted-Davis EA, Borrás T. Matrix GLA protein function in human trabecular meshwork cells: inhibition of BMP2-induced calcification process. *Invest Ophthalmol Vis Sci*. 2006;47:997–1007.
15. Madisen L, Zwingman TA, Sunkin SM, et al. A robust and high-throughput Cre reporting and characterization system for the whole mouse brain. *Nat Neurosci*. 2010;13:133–140.
16. Buie LK, Karim M, Smith MH, Borrás T. Development of a model of elevated intraocular pressure in rats by gene transfer of bone morphogenetic protein 2. *Invest Ophthalmol Vis Sci*. 2013;54:5441–5455.
17. Mitra RN, Gao R, Zheng M, et al. Glycol chitosan engineered autoregenerative antioxidant significantly attenuates pathological damages in models of age-related macular degeneration. *ACS Nano*. 2017;11:4669–4685.
18. Mitra RN, Nichols CA, Guo J, et al. Nanoparticle-mediated miR200-b delivery for the treatment of diabetic retinopathy. *J Control Release*. 2016;236:31–37.
19. Han Z, Conley SM, Makkia RS, Cooper MJ, Naash MI. DNA nanoparticle-mediated ABCA4 delivery rescues Stargardt dystrophy in mice. *J Clin Invest*. 2012;122:3221–3226.
20. Lambert V, Lecomte J, Hansen S, et al. Laser-induced choroidal neovascularization model to study age-related macular degeneration in mice. *Nat Protoc*. 2013;8:2197–2211.
21. Mitra RN, Han Z, Merwin M, Taai MA, Conley SM, Naash MI. Synthesis and characterization of glycol chitosan DNA nanoparticles for retinal gene delivery. *ChemMedChem*. 2014;9:189–196.
22. Mitra RN, Merwin MJ, Han Z, Conley SM, Al-Ubaidi MR, Naash MI. Yttrium oxide nanoparticles prevent photoreceptor death in a light-damage model of retinal degeneration. *Free Radic Biol Med*. 2014;75:140–148.
23. Hale JE, Fraser JD, Price PA. The identification of matrix Gla protein in cartilage. *J Biol Chem*. 1988;263:5820–5824.
24. Boström K. Insights into the mechanism of vascular calcification. *Am J Cardiol*. 2001;88:20E–22E.
25. Ramírez JM, Salazar JJ, Hoz Rd, et al. Choroidal vessel wall: hypercholesterolaemia-induced dysfunction and potential role of statins. In: Sugi H, ed. *Current Basic and Pathological Approaches to the Function of Muscle Cells and Tissues—From Molecules to Humans*. Rijeka, Croatia: InTech; 2012: 255–298.
26. Canfield AE, Doherty MJ, Kelly V, et al. Matrix Gla protein is differentially expressed during the deposition of a calcified matrix by vascular pericytes. *FEBS Lett*. 2000;487:267–271.
27. Alvarado J, Murphy C, Juster R. Trabecular meshwork cellularity in primary open-angle glaucoma and nonglaucomatous normals. *Ophthalmology*. 1984;91:564–579.
28. Alvarado J, Murphy C, Polansky J, Juster R. Age-related changes in trabecular meshwork cellularity. *Invest Ophthalmol Vis Sci*. 1981;21:714–727.
29. Battista SA, Lu Z, Hofmann S, Freddo T, Overby DR, Gong H. Reduction of the available area for aqueous humor outflow and increase in meshwork herniations into collector channels following acute IOP elevation in bovine eyes. *Invest Ophthalmol Vis Sci*. 2008;49:5346–5352.
30. Lu Z, Overby DR, Scott PA, Freddo TF, Gong H. The mechanism of increasing outflow facility by rho-kinase inhibition with Y-27632 in bovine eyes. *Exp Eye Res*. 2008; 86:271–281.
31. Vranka JA, Acott TS. Pressure-induced expression changes in segmental flow regions of the human trabecular meshwork. *Exp Eye Res*. 2017;158:67–72.
32. Wirostko BM. The vascular theory in glaucoma. *Glaucoma Today*. 2009;April:24–27.
33. Choi J, Kook MS. Systemic and ocular hemodynamic risk factors in glaucoma. *Biomed Res Int*. 2015;2015:9.
34. Huck A, Harris A, Siesky B, et al. Vascular considerations in glaucoma patients of African and European descent. *Acta Ophthalmol*. 2014;92:e336–e340.
35. Hui F, Nguyen CT, Bedggood PA, et al. Quantitative spatial and temporal analysis of fluorescein angiography dynamics in the eye. *PLoS One*. 2014;9:e111330.
36. Iljin K, Petrova TV, Veikkola T, Kumar V, Poutanen M, Alitalo K. A fluorescent Tie1 reporter allows monitoring of vascular development and endothelial cell isolation from transgenic mouse embryos. *FASEB J*. 2002;16:1764–1774.
37. Schallek J, Geng Y, Nguyen H, Williams DR. Morphology and topography of retinal pericytes in the living mouse retina using in vivo adaptive optics imaging and ex vivo characterization. *Invest Ophthalmol Vis Sci*. 2013;54:8237–8250.
38. Matsushita J, Inagaki S, Nishie T, et al. Fluorescence and bioluminescence imaging of angiogenesis in flk1-nano-lantern transgenic mice. *Sci Rep*. 2017;7:46597.
39. Schurgers LJ, Uitto J, Reutelingsperger CP. Vitamin K-dependent carboxylation of matrix Gla-protein: a crucial switch to control ectopic mineralization. *Trends Mol Med*. 2013;19:217–226.
40. Abe T, Fujimori T. Reporter mouse lines for fluorescence imaging. *Dev Growth Differ*. 2013;55:390–405.
41. Vacaru AM, Vitale J, Nieves J, Baron MH. Generation of transgenic mouse fluorescent reporter lines for studying hematopoietic development. *Methods Mol Biol*. 2014;1194: 289–312.

Investigative Ophthalmology & Visual Science